

## Advanced earth grid monitoring for HV network safety compliance

Mohamad Nassereddine, Ali Hellany, Jamal Risk, Tosin Famakinwa & Mahmood Nagria

To cite this article: Mohamad Nassereddine, Ali Hellany, Jamal Risk, Tosin Famakinwa & Mahmood Nagria (14 Oct 2024): Advanced earth grid monitoring for HV network safety compliance, Australian Journal of Electrical and Electronics Engineering, DOI: [10.1080/1448837X.2024.2414476](https://doi.org/10.1080/1448837X.2024.2414476)

To link to this article: <https://doi.org/10.1080/1448837X.2024.2414476>



© 2024 The Author(s). Published by Informa UK Limited, trading as Taylor & Francis Group.



Published online: 14 Oct 2024.



Submit your article to this journal [↗](#)



Article views: 222



View related articles [↗](#)



View Crossmark data [↗](#)

# Advanced earth grid monitoring for HV network safety compliance

Mohamad Nassereddine<sup>a</sup>, Ali Hellany<sup>b</sup>, Jamal Risk<sup>b</sup>, Tosin Famakinwa<sup>b</sup> and Mahmood Nagria<sup>b</sup>

<sup>a</sup>Department of Electrical, Computer and Telecommunication Engineering, University of Wollongong in Dubai, Dubai, United Arab Emirates; <sup>b</sup>School of Engineering Design and Built Environment, Western Sydney University, Kingswood Sydney NSW, Australia

## ABSTRACT

Electrical energy is a critical component for human comfort, but mismanagement of this energy can lead to human injury and even fatalities. High voltage safety compliance hinges on the presence of an adequate earthing system within the infrastructure. Various factors influence the effectiveness of the earthing system, including soil resistivity in the surrounding area and the availability of auxiliary paths for fault currents. Weather conditions, changes in the surrounding environment, and alterations within the high-voltage network significantly impact these elements. Any modifications to the auxiliary path conditions can have severe consequences on the network's safety compliance. The current industry practice lacks continuous monitoring of the earth grid and fault current paths, with no provision for frequent current injection tests on the entire earth grid system. To close the existing gap, this paper proposes a novel approach through the introduction of an Earthing IoT Monitoring system. This system enables network owners to monitor safety compliance across the entire network, identify fault current return paths, and pinpoint any necessary preventive maintenance measures. The paper also delves into the crucial roles played by soil resistivity and split factors in the earthing system domain. A case study is included to support the innovative nature of the proposed system.

## ARTICLE HISTORY

Received 9 April 2024  
Accepted 5 September 2024

## KEYWORDS

Earthing IoT; grounding;  
fault current; split factor;  
EPR; step and touch voltages

## 1. Introductions

In today's world, the reliance on electrical infrastructure is growing due to the increasing population. Limited land size often necessitates the proximity of electrical infrastructure to residential properties. Safety is paramount throughout the design, installation, commissioning, and operation of any system. In the realm of electrical infrastructure, safety can be ensured through proper earthing, lightning protection, and electrical protection systems. Safety breaches may manifest as step and touch voltages, typically stemming from faults or system malfunctions (Celin 2015; Colella et al. 2016; Zizzo et al. 2015). While electrical energy provides significant comfort to humans, any fault or malfunction can result in fatalities or permanent damage. The human body can only withstand a limited amount of electrical energy for a brief period, typically in milli-amperes. This places a responsibility on designers and researchers to maintain a robust system throughout its operational lifespan. Designers strive to establish a secure path for fault conditions back to the source (Nassereddine et al. 2014b; Nassereddine et al. 2013a), which may involve directing the fault current to Earth or a return conductor (Buccheri and Mangione 2008)

The magnitude of the fault current can exceed the load current by more than 10 times (Coppo et al. 2019). To ensure that the voltage rise stays below dangerous levels, the high current must be absorbed by a low-resistance path (Dladla, Nnachi, and Tshubwana 2022; Lee and Chang 2005). Introducing a conductive transmission structure near residential areas increases the risk of electric shock through step and touch voltages (Neitzel 2016; Thomas 2012; Walsh 2005). The soil resistivity structure of the surrounding area heavily influences the low-resistance path, known as the earth grid or grounding, at the fault location (Denche et al. 2021; Hellany et al. 2011; IEEE 81–2012; IEEE 80–2013; Malanda et al. 2018; Nassereddine et al. 2014a; Olowofela, Jolaosho, and Badmus 2005; Sazali et al. 2020; Stracqualursi, Araneo, and Mitolo 2021). This influence can potentially raise or lower the earth grid resistance when the soil resistivity structure changes, leading to a corresponding change in the voltage rise at the location. The alteration in earth grid resistance affects the split factor of the earthing system, which in turn impacts AC interference on nearby conductive structures (Nassereddine, Rizk, Hellany, et al. 2015; Micu, Christoforidis, and Czumbil 2013). Additionally, changes in the earth grid necessitate adjustments to the protection requirements of the system (AS/NZS 3851–1991).

**CONTACT** Mohamad Nassereddine  mohamadnassereddine@uowdubai.ac.ae

© 2024 The Author(s). Published by Informa UK Limited, trading as Taylor & Francis Group.

This is an Open Access article distributed under the terms of the Creative Commons Attribution-NonCommercial-NoDerivatives License (<http://creativecommons.org/licenses/by-nc-nd/4.0/>), which permits non-commercial re-use, distribution, and reproduction in any medium, provided the original work is properly cited, and is not altered, transformed, or built upon in any way. The terms on which this article has been published allow the posting of the Accepted Manuscript in a repository by the author(s) or with their consent.

As outlined in the provided information, the safety compliance of the electrical network is contingent upon various factors, including the soil composition of the surrounding environment. Changes in land use, such as in heavily developed areas, can lead to soil contamination that affects soil resistivity and may compromise the integrity of the earthing system, posing risks to nearby residential properties. It is evident from the discussion that continuous monitoring of the earthing system is crucial to ensure compliance throughout its operational lifespan. To achieve this, the implementation of smart monitoring mechanisms leveraging technological advancements, particularly in the realms of IoT and machine learning, is imperative. The paper delves into the soil resistivity structure, the earth grid of the electrical network, and the distribution of fault currents. It highlights the pivotal role that IoT and machine learning technologies can play in enhancing the safety standards of the electrical system. The research establishes the essential prerequisites for an effective IoT system and elucidates how it can be integrated with machine learning to uphold system safety without disrupting its functionality.

## 2. Electrical earthing system

This section discusses the following:

- Soil resistivity structure
- Safety and soil resistivity
- Earth grid
- Distributions of fault current
- Discussion

### 2.1. Soil resistivity structure

The earth grid will be surrounded by a soil resistivity structure with varying values, which are dependent on the soil type. Soil resistivity values can range from 2 to 100,000  $\Omega.m$ , with more extreme values not uncommon. Table 1 provides a breakdown of resistivity values for different ground conditions.

### 2.2. Safety and soil resistivity

Electrical power, inherently, poses a risk of harm to humans in the event of a fault or mishandling of

equipment. The primary danger to individuals is the possibility of power current passing through the heart, which can lead to ventricular fibrillation depending on the current magnitude. Two globally accepted approaches are in place to address this risk:

- IEC standard derived by Beilgelmeir, which was also published in AS/NZS 60,479:2010 (IEC/TS60479-1)
- IEEE standard which Dalziel derives is published in IEEE80 and ENA EG1

These standards define the permissible current level in the human body in relation to clearance time. IEEE 80 categorises individuals into two groups based on weight: 50 kg for evaluating safety limits in publicly accessible areas and 70 kg for evaluating safety limits in restricted areas. According to IEEE (IEEE 81–2012; IEEE 80–2013), the permissible safety limits are outlined in Table 2. This table differentiates between the two body types and the allowable touch voltage for metal-to-metal contact.

Where,

$t$  is the duration of the shock current (in seconds)

$\rho_s$  is the resistivity of the surface material (Ohm.m) – soil or crushed rock. In areas where grid conductors are directly exposed, such as an earthed steel reinforced concrete floor, the surface resistivity is considered to be zero. This assumption also applies to hand-hand prospective touch voltages or touch voltages near an earth grid, like the concrete above-reinforced steel connected to an earth grid.

**Table 1.** Typical soil resistivities of various types of soil (Hellany et al. 2011; IEEE 81–2012).

Type of Soil or water	Typical Resistivity ( $\Omega.m$ )
Sea Water	2
Clay	40
Ground well and spring water	50
Clay and Sand mix	100
Shale, Slates, Sandstone	120
Peat, Loam, and Mud	150
Lake and Brook Water	250
Sand	2000
Morane Gravel	3000
Ridge Gravel	15000
Solid granite	25000
Ice	100000

**Table 2.** IEEE allowable safety limits.

Body Type	Prospective Touch Voltage (V)	Prospective Step Voltage (V)
50kg body mass (Publicly accessible areas)	$= \left(\frac{0.116}{\sqrt{t}}\right)(1000 + 1.5C_s\rho_s)\rho$	$= \left(\frac{0.116}{\sqrt{t}}\right)(1000 + 6C_s\rho_s)$
70kg body mass (Restricted areas within a substation)	$= \left(\frac{0.152}{\sqrt{t}}\right)(1000 + 1.5C_s\rho_s)$	$= \left(\frac{0.152}{\sqrt{t}}\right)(1000 + 6C_s\rho_s)$
50kg body mass (public accessible areas)	$= \left(\frac{0.116}{\sqrt{t}}\right)$ Metal to Metal	
70kg body mass (Restricted areas within a substation)	$= \left(\frac{0.152}{\sqrt{t}}\right)$ Metal to Metal	

$C_s$  is the derating factor relating to surface layer thickness and resistivity and can be found using equation 1

$$C_s = 1 - \frac{0.09 \left(1 - \frac{\rho}{\rho_s}\right)}{2h_s + 0.09} \quad (1)$$

Where

$h_s$  is the depth of the surface layer

$\rho$  is the apparent soil resistivity

### 2.3. Earth grid

The grid resistance value plays a crucial role in the safety impediment of the designed system. The soil structure discussed in the previous section is a key factor in determining the accurate grid resistance. The earth's grid resistance, in conjunction with the fault current within the grid, dictates the earth's potential rise at the grid location. The earth grid of an earthing system comprises the following components:

- Single electrode
- Multiple electrodes, if the single electrode system is not competent to accomplish the requisite outcomes
- Mesh grid
- Combination of mesh and electrode grid

Numerous standards and research efforts aim to develop formulas for calculating the resistance of a designated earth grid, based on IEEE (IEEE 81–2012; IEEE 80–2013) equation 2 to calculate the earth grid. This equation solely focuses on the grid's area and does not account for the type or length of the ground conductor.

$$R_g = \frac{\rho}{4} \sqrt{\frac{\pi}{A}} \quad (2)$$

Where

$R_g$  is the ground grid resistance in ohms

$\rho$  is the soil resistivity in ohm.m

$A$  is the area occupied by the earth grid in  $m^2$

### 2.4. Fault current distribution

The split factor indicates the portion of the faulted current that utilises the substation earth grid. Equations 3 and 4 illustrate the connection between the split factor and the substation fault current, as well as the OHEW (Overhead Earth Wire) return fault current. Analysing the circuit in Figure 1 enables the determination of the split factor. The evaluation can be conducted with or without considering the mutual impedance of the OHEW.

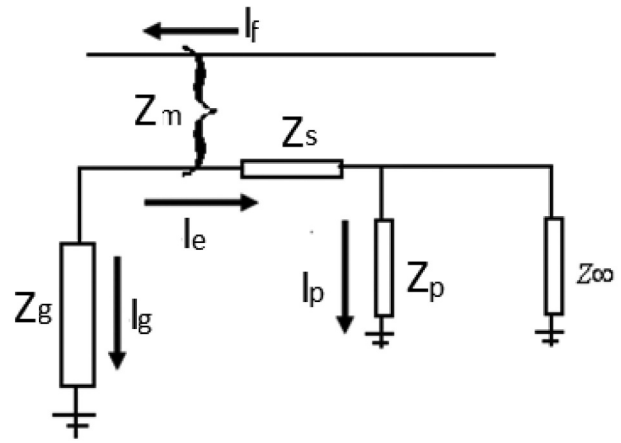


Figure 1. Split factor circuit analysis.

$$I_g = I_f \times \delta_f \quad (3)$$

$$I_e = I_f (1 - \delta_f) \quad (4)$$

Where

$I_g$  is the fault current in the substation earth grid

$\delta_f$  is the split factor

## 3. Discussions

Safety is always a top priority in any global activity or project. Improper management of electricity can result in serious harm to individuals. As detailed in the preceding sections, human safety is influenced by various factors, including soil resistivity and the condition of the earthing system. Soil resistivity fluctuates with changes in the environment or surrounding infrastructure, impacting permissible step and touch voltage safety thresholds, earth grid resistance, and fault current distribution. It is unfeasible to have a single soil structure covering the entire electrical network, and accurately predicting soil structure for a specific area within the network is challenging. The interconnected nature of the electrical network allows fault currents to flow through any suitable path back to the source. During the design and commissioning phases of electrical infrastructure, designers aim to address worst-case scenarios based on available data at the project's inception. Continuously adapting to surrounding changes affecting the earthing system and safety demands significant workforce resources, substantial budget allocations, and planned network outages. To mitigate these challenges and minimise costs, complexity, and disruptions, deploying IoT with Machine Learning (ML) for ongoing system monitoring, particularly in newly developed areas, is a practical solution.

## 4. IoT and machine learning role

In recent years, the world has witnessed a sharp increase in IoT deployments, capability, and security. The ability of the IoT to collect accurate data regarding current, voltage, and power, allows it to be a perfect tool to monitor the fault current across the network. During the construction of a new area, incorporating IoT into all high-voltage earthing systems ‘shouldn’t be a major issue as it is already used in all the power system sections (Bedi et al. 2018; Mansour et al. 2023; Radhakrishnan and Gopalakrishnan 2020). The current research shows the ability of ML to analyse IoT data and issue reports, instructions, and decisions at high accuracy (Khatoon, Dilshad, and Song 2022; Mishra and Tyagi 2022), making IoT even more attractive for the proposed tasks under this paper.

### 4.1. IoT proposed locations

In this paper, the following IoT are deployed as per Table 3.

It is worth noting that the deployed IoT must have the following characteristics as a minimum:

- Ability to withstand high voltage; maximum voltage level must be defined by the utility
- Ability to measure high current and voltage accurately. It is worth noting that all readings have errors, however, this paper is to show the advanced role that IoT can play in advancing the safety standards of the electrical network. therefore, the scope of the paper doesn’t include the error percentage of the reading.
- Ability to complete the measurements within a small part of the cycle. For this project, the collection rate is considered to have a 2 millisecond gap (Elsts et al. 2016).

In the current power system market, the accuracy of current and voltage measurement devices is reliable and widely used across the network. While this paper’s scope does not specifically address the quality and accuracy of the reading sensors, it is based on previously utilised equipment to support the proposed theory.

For instance, at the padmount substation, current data will be gathered using a CT (current transformer). Similarly, data will be collected at

other substations. In terms of voltage measurement, a transducer with a capability of several thousand volts and a range of calibration options to suit the desired environment can be utilised. Additionally, at pole locations, a current transducer can be employed to collect current data.

### 4.2. ML capability and requirements

The electrical network covers a vast area and comprises tens of thousands of high-voltage infrastructures. It is not feasible for humans to monitor the signals from the network and issue instructions. Nevertheless, the increasing capabilities of machine learning algorithms enable quick, dependable, and effective monitoring and management of electrical network data. The role of machine learning in this paper encompasses:

- Collect data from the electrical power network. The data includes the following as a minimum
  - (a) Load current
  - (b) Fault locations and its details
  - (c) System ’ malfunction’s locations and details
- Collect data from the earthing system IoT
- Analyse the big data, remove bad data, allocate data to the nominated sector
- Keep comparing the measured current into the earth grid to the designed one. Also, link it to the fault in the network
- Issue reports if the measured data is within the safe limit. The operator will set the safe limit
- Issue an urgent warning if the measured data is outside the safe limit.
- Ability to map the fault current route throughout the years and identify any deviation

#### 4.2.1. Benefits of ML

The current literature review supports ML’s high capability in data analysis and decision-making within the electrical network (Cheng and Yu 2019; Goswami and Roy 2019; Ibrahim, Dong, and Yang 2020; Mocanu, Nguyen, and Gibescu 2018). This capability along with the IoT offers a wide range of benefits for the safety compliance of the electrical network. The ability to continuously analyse

**Table 3.** Location of earthing IoT.

IoT Type	Installation Location	Main Role
Current Measurements	<ul style="list-style-type: none"> <li>• 11kV/415 V substation earth grid</li> <li>• HV cable screen termination</li> <li>• HV pole down conductor</li> </ul>	Ongoing current measurements and sending it for assessment
Voltage Measurements	Earth grid where there is a reference zero point*	Ongoing voltage measurements and send them for assessment

\*The zero-point reference could be present by a spare copper communication line that can be earthed at the other end.

collected data and map the fault current route across the network offers the setup of an accurate virtual earthing network. For the path that is more impacted by fault current, the operator will set more frequent maintenance inspections to avoid any unwanted safety breaches. This preventive maintenance advances network safety standards and extends the infrastructure's operating life. Furthermore, the analysis can extend to predict and highlight any potential earthing failure. This can be achieved by continuously analysing and comparing with old data, when a fault current magnitude is the same; however, its path starts to change without any information of major ground disturbance (development), the ML can issue a warning or an investigation task to the operator to inspect. This change in the current path could be a factor in electrode damage or OHEW connection failure.

## 5. Electrical network and earthing IoT

The electrical network covers a large area and includes thousands of high voltage infrastructure. Under a fault current at any given location, the current magnitude could search to reach thousands of amperes. This high current must find its way back to the source using the least resistive path. In this section, the complexity of the large network is shown. Also, the layout shows the proposed location of the IoT along the network and its significance when it comes to safety compliance.

### 5.1. Fault current and grid resistance

IoT devices are heavily used in the power network. Table 4 contains collected data from the electrical generator system (Gebrael et al. 2004; Mohapatra et al. 2023; Mohapatra, Mohanty, and Tripathy 2024; Shi et al. 2020). The table supports IoT capability in collecting accurate measurements. The paper's initiative is to collect current data and monitor the current path under system fault. Also, IoT voltage

**Table 4.** Collected data using IoT sensors (Gebrael et al. 2004; Mohapatra et al. 2023; Mohapatra, Mohanty, and Tripathy 2024; Shi et al. 2020).

Parameters collected	Parameters collected
Particulate Matter	Voltage
Sulfur Dioxide	Current
Oxides of nitrogen	Frequency
Carbon Monoxide	Power
Oxygen	Harmonics
Non-Methane Hydro-Carbon	Coolant temperature
Engine vibration	Engine Speed
Noise level	Fuel Level
Engine Temperature	Oil Pressure
Generator status	Battery voltage
Fault conditions	Fault data

measurements allow for continuous measurement of the earth's potential rise and the grid resistance as of the known infrastructure. The devices can collect fast measurements, in microsecond increments, for fault current (Auzanneau 2018). The fault current clearance time reaches multiple cycles, more than 150 milliseconds, which makes measurements in microsecond increments suitable for accurate captures of fault current data (Cheng and Yu 2019; Li et al. 2012)

To analyse the fault current path, equation 5 is proposed in this work. The equation is based on the nodal theorem: the exiting current (Fault current generated) must equal the entering current (the current into the earth grid system):

$$\sum_{i=1}^N I_oT_{Ei} = \sum_{k=1}^M I_oT_{Fk} \quad (5)$$

Where

$I_oT_{Ei}$  is the current measured by the earth-IoT at location  $i$

$I_oT_{Fk}$  is the fault current measured by the power system at a location  $k$

For more details analysis, the paper introduces equation 6 to distinguish between cable screen, OHEW, and earth grid fault current.

$$\sum_{i=1}^N I_oT_{Ei} = \sum_{i=1}^N I_oT_{ESCi} + \sum_{i=1}^N I_oT_{EOHi} + \sum_{i=1}^N I_oT_{Egi} \quad (6)$$

Where:

$\sum_{i=1}^N I_oT_{ESCi}$  is the Fault current measured by the cable screen IoT at location  $i$

$\sum_{i=1}^N I_oT_{EOHi}$  is the fault current measured by the OHEW IoT at location  $i$

$\sum_{i=1}^N I_oT_{Egi}$  is the fault current measured in the earth grid IoT at location  $i$

Equation 6, along with the voltage measurement IoT, helps measure the EPR (Earth Potential Rise) and earth grid location at the IoT location. To measure the EPR and earth grid resistance, a zero-reference point is required. This can be achieved by using a spare communication wire terminated at a remote area (Coppo et al. 2019; IEEE 80–2013; Nassereddine et al. 2013b; Nassereddine, Rizk, Nagrial, et al. 2015). The paper introduces equation 7 to compute the earth grid resistance at location ' $i$ ' when the voltage IoT is present.

$$R_{gi} = \frac{I_oT_{Vi}}{I_oT_{Egi}} \quad (7)$$

Where

$I_oT_{Vi}$  is the measured voltage by the IoT located at location ' $i$ '

It is also possible to estimate the input impedance including the mutual impedance if applicable for a cable screen and OHEW. Equation 8 can be used to determine the input impedance of the cable screen and OHEW at location 'i'.

$$R_{Ei} = \frac{IoT_{Vi}}{IoT_{ESCi} + IoT_{EOHi}} \quad (8)$$

## 5.2. Data from IoT & return path

Figure 2 shows a sample network that covers a large metropolitan area. The network includes the 330kV and 132kV transmission networks. The

earthing system for the entire network can be connected using OHEW, OPGW (Optical Ground Wire), or a high-voltage cable screen. Figure 3 shows a distribution network connected to one of the 132kV substations. The 132kV/11kV is feeding a large number of padmount substations. These 11kV padmounts earth grid are connected to the 132kV/11kV substation earth grid using the HV cable screen.

Under a fault condition, the fault current must find its way back to the transformer source. The current finds the least resistive way back to the source. As discussed in the introduction and theoretical section,

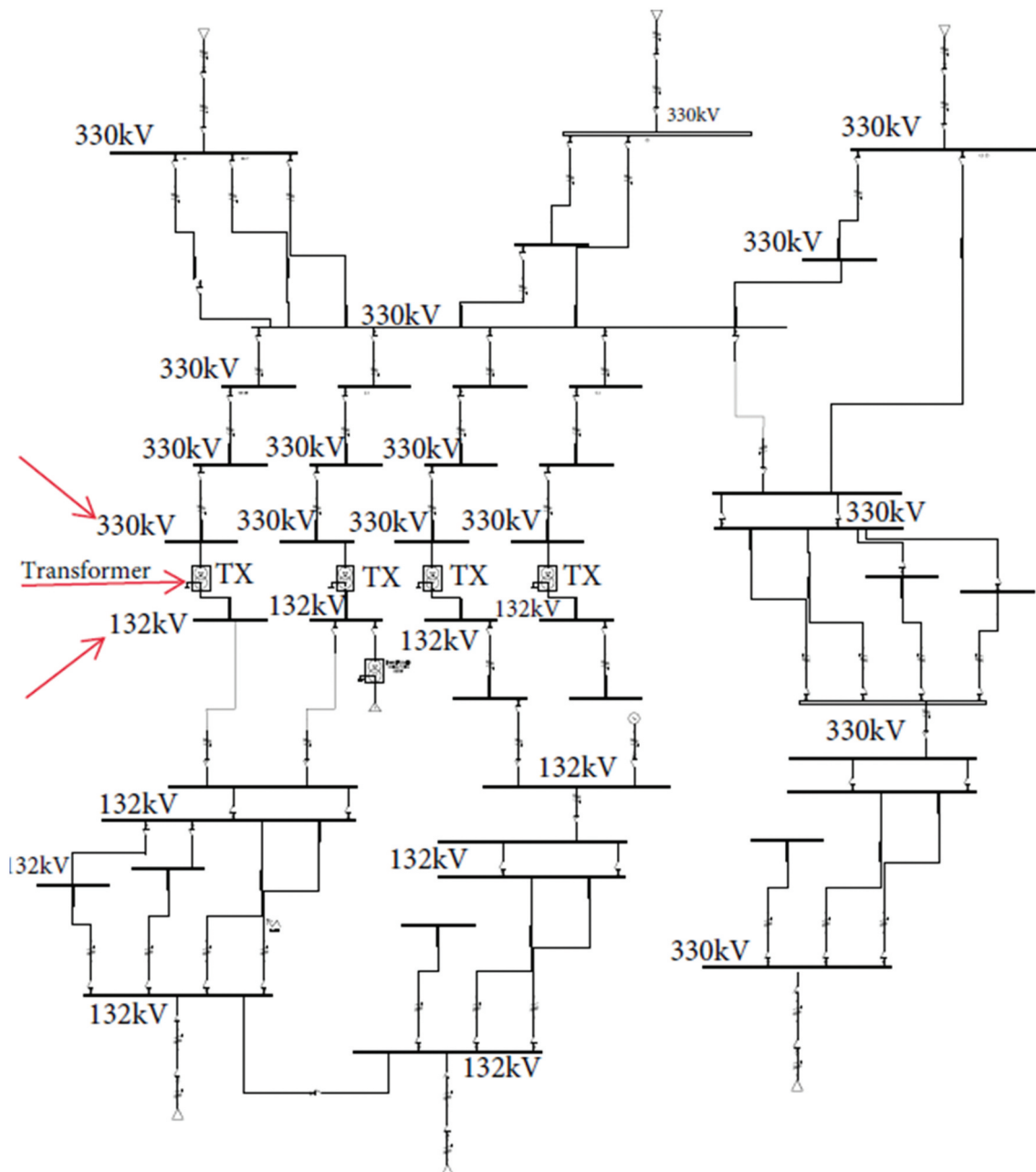
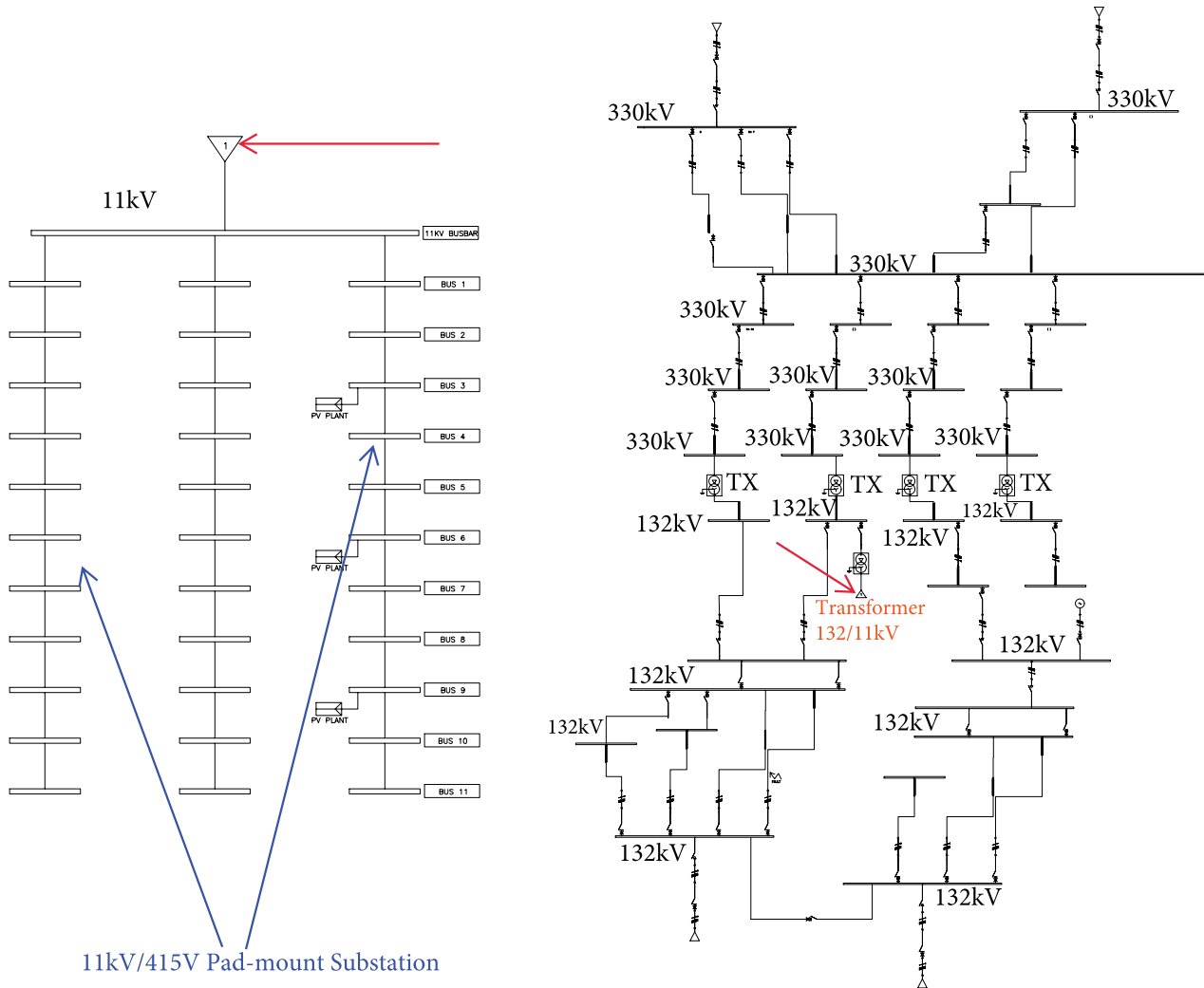


Figure 2. Complex 330kV and 132kV network.



**Figure 3.** The distribution network connected to one of the 132kV substations.

the coupling factor also is important. **Figure 4** illustrates a fault current located along the network. The red section shows the possible return path back to the sourced transformer. The distribution fault current could utilise the earth grid system at each pad-mount, 11kV HV cable screen, and 132kV/11kV substation earth grid on its way back to the source. This utilisation introduces the earth potential rises at each pad-mount substation. Under the condition that the 11kV network is newly established, it is impossible to run a current injection test to determine the fault current impact on these 11kV under all possible fault locations along the entire network.

To eliminate the risk of non-compliance to earth grid requirements, the installation of earthing IoT as proposed in this paper, allows for ongoing monitoring of the fault current path and any generated earth potential rise. Based on **Figures 2 and 3**, it is clear that the quantity of IoT will be large. The large number of IoT sensors reflects a large number of input data that could exceed hundreds of gigabytes daily.

It is worth noting that this paper's aim is not to address the machine learning capability to manage big

data. However, it aims to highlight the important role of IoT in HV earthing to ensure safety compliance by ongoing monitoring of the fault's current path. Under this paper, machine learning performs the following tasks:

- Eliminate bad data
- Allocate data to each sector, for example, fault current to the fault current folder, earth grid current to its folder, cable screen or OHEW current to its folder, and the voltage measurements to its folder.
- Complete assessments based on equations 5, 6, 7, and 8
- Determine the EPR and the grid resistance at nominal locations.
- Compare the values with the designed or safety limits.
- Issue reports and recommendations.

From **Figure 4**, the Earth IoT sensors recorded current at the following locations:

- At the faulted feeder



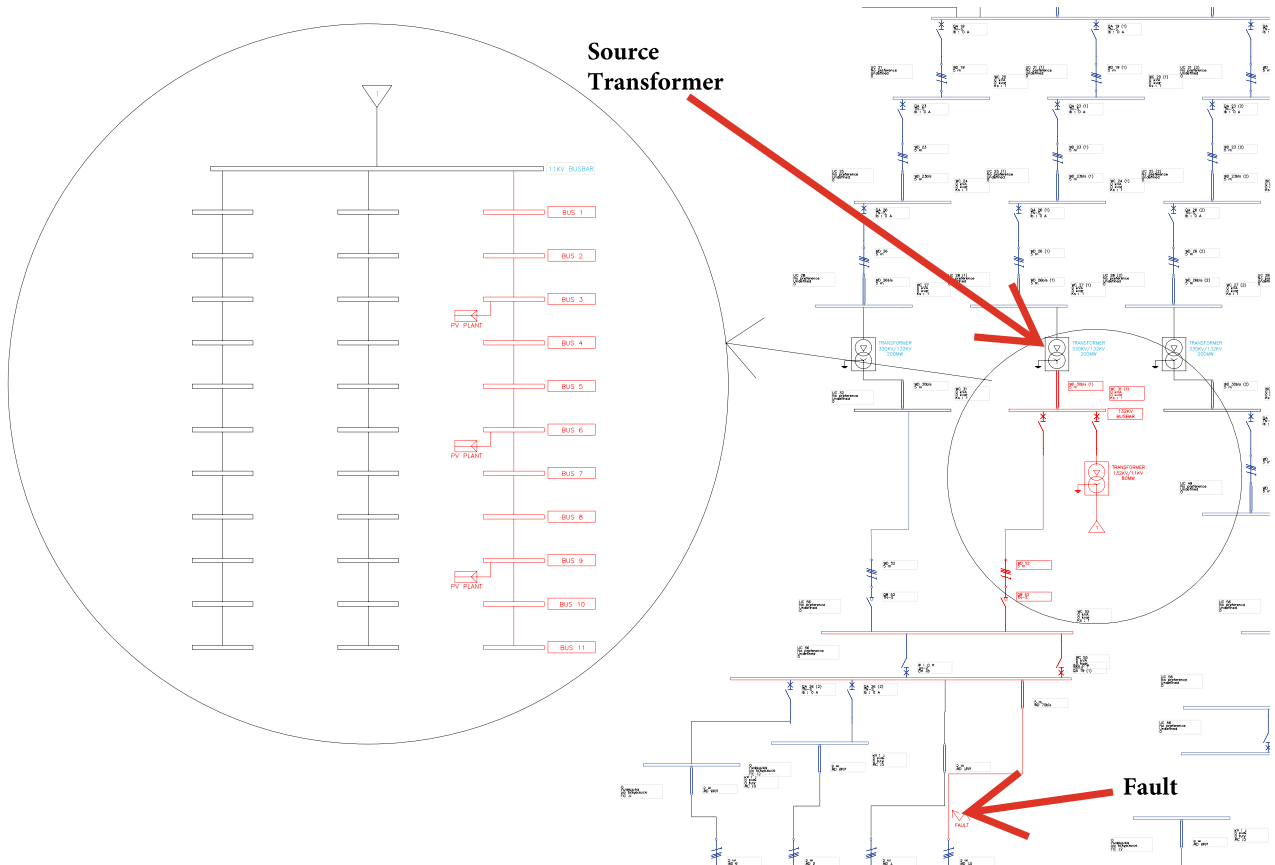


Figure 4. Fault location and possible return path back to the source transformer.

- Bus-y
- Bus-x
- Each pad-mount substation is highlighted in red
- The feeder that connects bus-y to bus-x

These records allow the system to identify the actual path that the fault current utilises as a return path

## 6. Case study

The case study is based on assessing different fault conditions and locations within the network shown in Figure 3. Figure 5 shows the proposed fault location along the network. The fault conditions are as follows:

- (1) F1 is a single line to ground fault at a substation, with a fault magnitude of 15 kA
- (2) F2 is a single line to ground fault at a substation, with a fault magnitude of 10 kA

- (3) F3 is a single line to ground fault along the 132kV feeder, with a fault magnitude of 10 kA
- (4) All substations have an earth grid resistance of 1 ohm
- (5) All transmission poles have a pole grid resistance of 10 ohms
- (6) Padmount substation earth grid of 3 ohms

It is important to highlight that the analysis conducted in this assessment was based on the author's previously published works and adhered to IEEE standards. These references can be utilised for the steps used in calculating the split factor, which determines the percentage of current flowing into the ground and the return path (Nassereddine et al. 2014b, IEEE 81–2012; IEEE 80–2013; Nassereddine 2024). Also, these references can be used to ensure that accurate soil data is obtained along with the earth grid resistance computation. To give a high-level explanation to readers, the following steps were completed during the analysis:

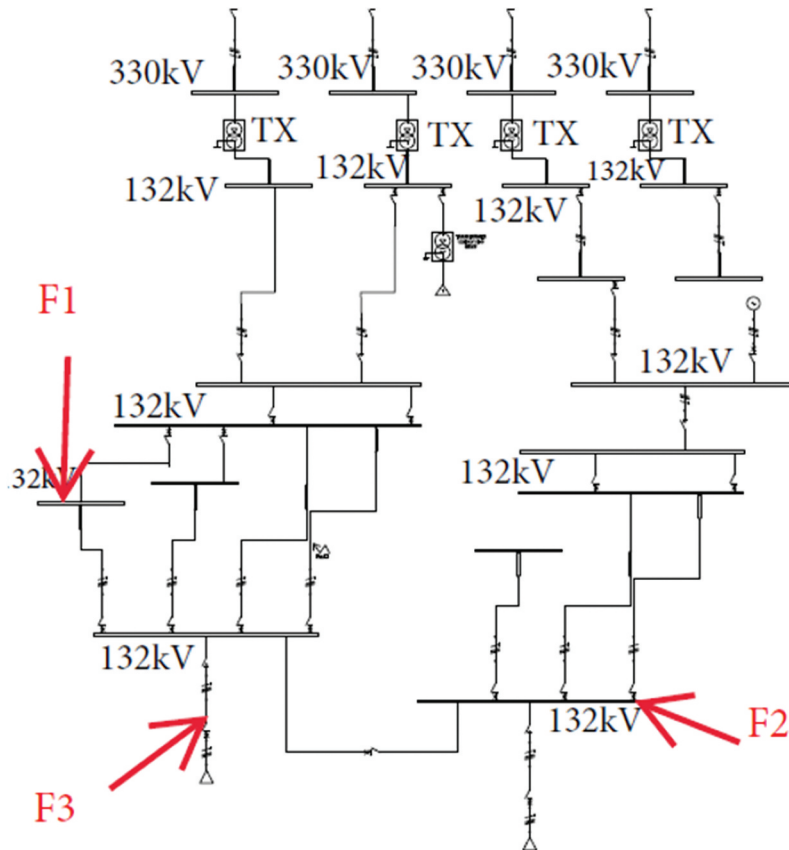


Figure 5. Location of faults along the network.

- Determined the split factor as per (Nassereddine et al. 2014b; IEEE 81-2012; IEEE 80-2013; Nassereddine 2024)
- Based on the found split factor, the author determined the current injected into the grid and the one used the auxiliary path.
- The author relied on (Nassereddine et al. 2014b; Nassereddine 2024) to find the current injected into each pole and padmount substation
- The author determined the EPR at the desired location

Figure 6-a shows the detected path for the fault at location F1, and the system shows the EPR along the location. In this case study, the fault at location F1, has found a 3120A is injected into the ground and the remaining fault current used a return path. The EPR at the fault location is 3120 V, while the EPR at the source substation is 1240 V. The current that returns using the earth grid at the source substation is 1240A, while the one that is injected into the ground at the faulted substation is 3120A. This means that 1970A found its way back to the source by climbing on another auxiliary path. That caused the EPR at the intermediate substation, EPR of 980 V, and along the

transmission-line network. For the fault at F1, no measurement is detected along the distribution network. Therefore, the 11kV distribution network was not impacted by a fault at F1.

The fault at location F2 impacts a wider network including multiple padmounts along the newly subdivided area. Table 5 reflected a picked location for the IoT that recorded a current measurement.

Table 5 shows that a fault at location F2 impacts the EPR at four pad-mount substations where two of these pad-mounts, the recorded EPR exceeds the designed value. A warning message will be shown on the control screen at the utility monitoring room, also a report will be emailed to the responsible officer. It is also possible for the system to set the maximum percentage that EPR can exceed the designed value before the faulted line is shut down for urgent earth grid modifications.

A fault at location F3 impacted a wider area. This part of the case study focuses on the impact of the F3 fault on the distribution network. Figure 7 shows the pad-mount that recorded fault current measurement and Table 6 shows the recorded data. The record allows for highlighting of the

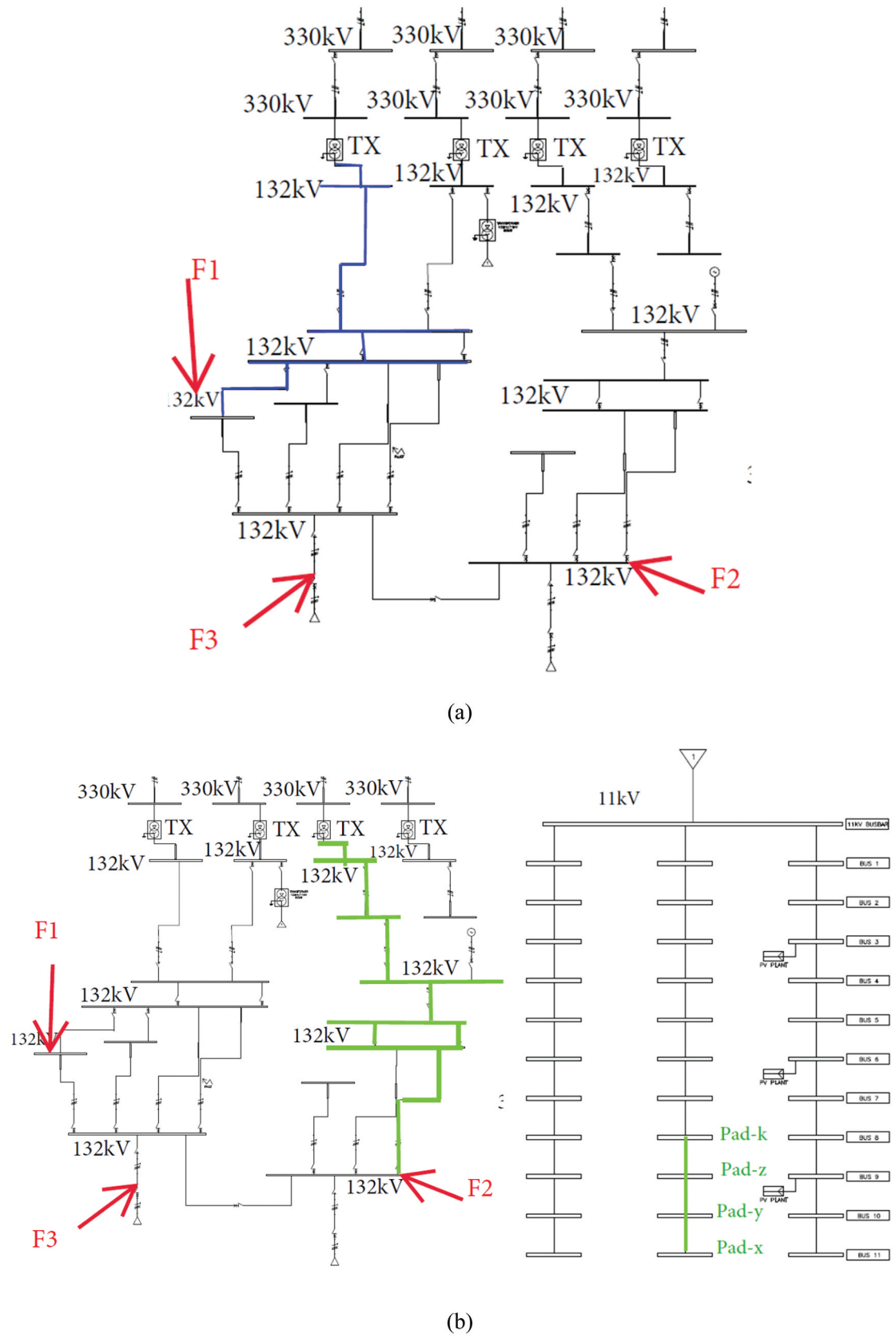


Figure 6. a) fault current path for a fault at F1 b) fault current path for a fault at F2 Location of faults along the network.

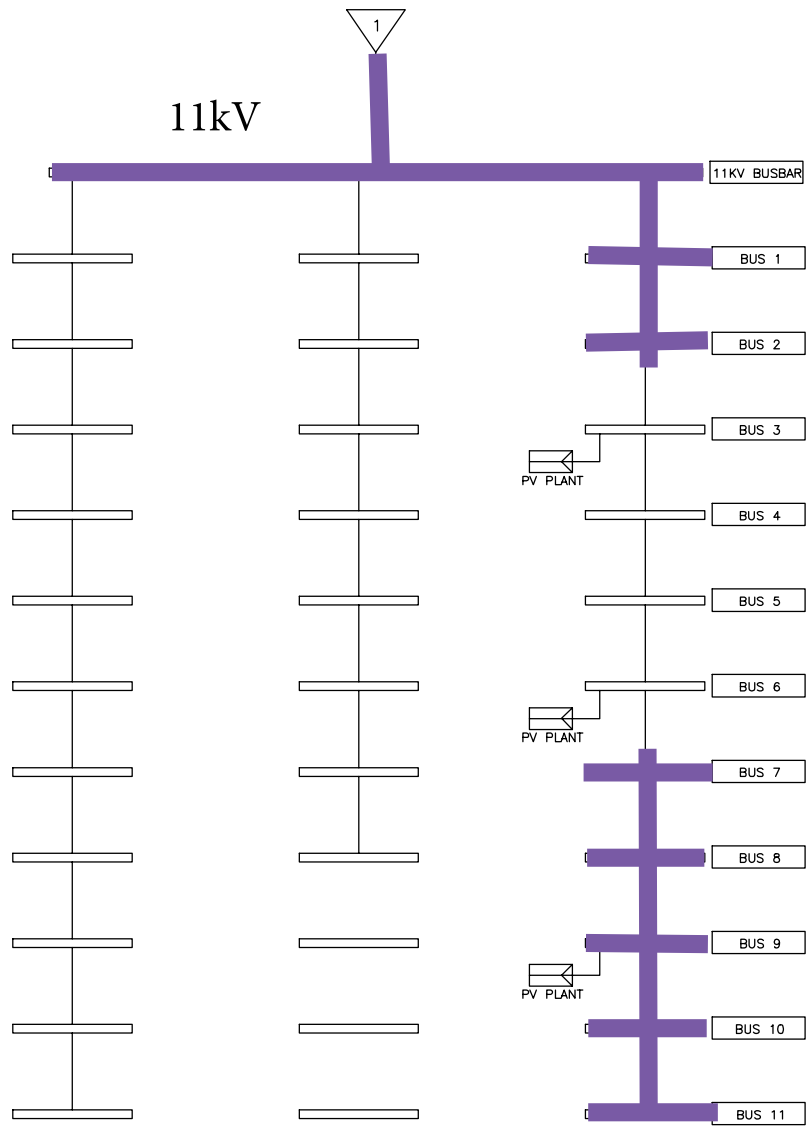


Figure 7. Shows the padmount substation that the Earth IoT measured the current.

Table 5. IoT measurements and EPR.

Fault Location	IoT Location	IoT Measurement	EPR at IoT location	Designed EPR	Comments
F2	Faulted substation	4230A	4230V	4900V	
F2	Intermediate Substation	1870A	1870V	2050V	
F2	Pad-x	210A	630V	600V	Attention required
F2	Pad-y	110A	330V	600V	
F2	Pad-z	150A	450V	600V	
F2	Pad-k	180A	540V	500V	Attention is required

Table 6. Record data on the padmount earth IoT.

Fault Location	IoT Location	IoT Measurement	EPR at IoT location	Designed EPR	Comments
F3	Sub-11	287A	861V	500V	Attention required
F3	Sub-10	186A	558V	500V	Attention required
F3	Sub-9	132A	396V	500V	
F3	Sub-8	90A	270V	500V	
F3	Sub-7	78A	234V	500V	
F3	Sub-2	127A	381V	500V	
F3	Sub-1	169A	507V	500V	Attention required
F3	11kV Busbar	18A	54V	500V	
F3	11kV Cable Screen	1165A			

path of the fault current and indicates which location needs attention to ensure the safety compliance of the designed elements.

## 7. Case study discussions

Safety is always the highest priority for electrical design, installation, commissioning, and operation. Due to the increased population, new areas are being developed and the electrical network is being altered. As shown in the case study, a new subdivision area involved the installation of two 11kV distribution feeders with a large number of padmount 11kV/415 V transformers to support the electrical load. The new HV infrastructure is located in the middle of the large network. Under fault along the network, the return current back to the source could utilise the newly installed HV infrastructure. This occurrence could happen even if the fault is located on a remote feeder that is not linked to the distribution substation.

It is also worth noting that under damage to OHEW or cable screen, the conditions of the EPR along the 11kV could increase, which increases the safety risks of the surrounding residential properties. Monitoring and completing monthly current injection (the CIT is the most commonly used method to test the earth grid compliance of the HV network) tests on the earth grid is not possible. However, following the proposed Earthing IoT concept under this paper allows for continuous monitoring of the system in addition to determining the actual fault current return path. This approach can be further developed to include the preventive maintenance ability of the system.

Under the mentioned case study, the locations of faults F2 and F3, impact the EPR at numerous pad-mount substations. As shown, the current injected into the earth grid generates an EPR higher than the designed one. The high EPR is located near a habitable area which could lead to human injury or fatality. The system detection and alarm could not have been possible without the support of the Earth IoT as proposed in this paper. From this approach, the work under this paper is considered novel as safety compliance cannot be maintained without following the proposed approach.

The current practice lacks the capability to conduct a comprehensive assessment of the entire local network and is unable to identify defects that may compromise the safety compliance of the system. In contrast, the proposed method makes significant contributions to the existing industry by addressing these limitations and enhancing overall system safety and compliance.

## 8. Conclusions

Electrical power infrastructure is expanding worldwide to support the increase in load demand. The electrical fault occurs at numerous locations, transmission lines, or substations, which could lead to a surge in current, which reflects a high earth potential rise at the faulted location or along its return path. The current available practice limits the monitoring of the fault current along its path. Also, it is not possible to carry out weekly or monthly current injection tests across the entire network under different weather conditions.

The novel proposed method in this paper, supported by the case study, allows for continuous monitoring of the earth's grid current under any fault along the network. The case study shows three different fault conditions and possible return paths. The result of the case study highlights the impacts that fault current could have on existing HV earth grid systems. Also, the proposed system identifies the location where safety compliance might be in concern. The proposed methods meet the advancements in technology, allow for ongoing monitoring, especially when the network is more complex, and ensure system safety compliance is maintained under different fault conditions.

The work also highlighted the possibility of the proposed method to team up with the advanced capability of machine learning to advance the analysis and issuing of reports and recommendations. This allows the high-voltage earth grid system to be prepared for the Industrial Revolution 4.0 and the complexity that comes with it.

## Disclosure statement

No potential conflict of interest was reported by the author(s).

## References

- AS/NZ 3851–1991. *The Calculation of Short-Circuit Currents in Three-Phase AC Systems*. Australia: Standards Australia.
- Auzanneau, F. 2018. "Detection and Characterization of Microsecond Intermittent Faults in Wired Networks." *IEEE Transactions on Instrumentation and Measurement* 67 (9): 2256–2258. <https://doi.org/10.1109/TIM.2018.2851646>.
- Bedi, G., G. K. Venayagamoorthy, R. Singh, R. R. Brooks, and K. C. Wang. 2018. "Review of Internet of Things (IoT) in Electric Power and Energy Systems." *IEEE Internet of Things Journal* 5 (2): 847–870. <https://doi.org/10.1109/JIOT.2018.2802704>.
- Buccheri, P. L., and S. Mangione. 2008. "Analysis of Ground Fault Current Distribution Along Nonuniform Multi-Section Lines." *Electric Power Systems Research* 78 (9): 1610–1618. <https://doi.org/10.1016/j.epsr.2008.02.001>.

- Celin, M. 2015. "Earth Fault Current Distribution on Transmission Networks." *Universita Degli Studi Di Padova*.
- Cheng, L., and T. Yu. 2019. "A New Generation of AI: A Review and Perspective on Machine Learning Technologies Applied to Smart Energy and Electric Power Systems." *International Journal of Energy Research* 43 (6): 1928–1973. <https://doi.org/10.1002/er.4333>.
- Colella, P., R. Napoli, E. Pons, R. Tommasini, A. Barresi, G. Cafaro, A. De Simone, et al. 2016. "Current Distribution During a Fault in an MV Network: Methods and Measurements." *IEEE Transactions on Industry Applications* 52 (6): 4585–4593. <https://doi.org/10.1109/TIA.2016.2600672>.
- Coppo, M., F. Bignucolo, R. Turri, H. Griffiths, N. Harid, and A. Haddad. 2019. "Analysis of Frequency Distribution of Ground Fault-Current Magnitude in Transmission Networks for Electrical Safety Evaluation." *Electric Power Systems Research* 173:100–111. <https://doi.org/10.1016/j.epsr.2019.03.024>.
- Denche, G., E. Faleiro, G. Asensio, and J. Moreno. 2021. "Grounding Electrodes with Internal Resistance: Application to Feasibility Study of the Driven-Rod Method for Modeling the Soil Electrical Resistivity Profile." *Applied Sciences* 11 (11): 5032. <https://doi.org/10.3390/app11115032>.
- Dladla, V. M. N., A. F. Nnachi, and R. P. Tshubwana. 2022. "Analysis of Design Parameters on Substation Earth Grid Safety Limits." *Science Publishing Group* 10 (2): 61–72.
- Elsts, A., S. Duquennoy, X. Fafoutis, G. Oikonomou, R. Piechocki, and I. Craddock. 2016. "Microsecond-Accuracy Time Synchronization Using the IEEE 802.15.4 TSCH Protocol." *Proceedings of the 2016 IEEE 41st Conference on Local Computer Networks Workshops (LCN Workshops)*, Dubai United Arab Emirate, 156–164. IEEE. November.
- Gabraeel, N., M. Lawley, R. Liu, and V. Parmeshwaran. 2004. "Residual Life Predictions from Vibration-Based Degradation Signals: A Neural Network Approach." *Transportation Industrial Electronic* 51 (3): 694–700. <https://doi.org/10.1109/TIE.2004.824875>.
- Goswami, T., and U. B. Roy. 2019. "Predictive Model for Classification of Power System Faults Using Machine Learning." *Proceedings of the TENCON 2019–2019 IEEE Region 10 Conference (TENCON)*, Kochi, India, 1881–1885. IEEE. October.
- Hellany, A., M. H. Nagrial, M. Nassereddine, and J. Rizk. 2011. "Soil Resistivity Structure and Its Implications on the Earth Grid of HV Substation." *World Academy of Science Engineering and Technology* 60: 1322–1326.
- Ibrahim, M. S., W. Dong, and Q. Yang. 2020. "Machine Learning Driven Smart Electric Power Systems: Current Trends and New Perspectives." *Applied Energy* 272:115237. <https://doi.org/10.1016/j.apenergy.2020.115237>.
- IEEE 80-2013. *IEEE Guide for Safety in AC Substation Grounding*. Australia: Standards Australia.
- IEEE 81-2012. 2012. *IEEE Guide for Measuring Earth Resistivity, Ground Impedance, and Earth Surface Potentials of a Grounding System*. USA: IEEE Standards.
- Khatoun, N., N. Dilshad, and J. Song. 2022. "Analysis of Use Cases Enabling AI/ML to IOT Service Platforms." *Proceedings of the 2022 13th International Conference on Information and Communication Technology Convergence (ICTC)*, Jeju Island, Republic of Korea, 1431–1436. IEEE. October.
- Lee, C. H., and C. N. Chang. 2005. "Computation of Current-Division Factors and Assessment of Earth-Grid Safety at 161/69 kV Indoor-Type and Outdoor-Type Substations." *IEEE Proceedings-Generation, Transmission and Distribution* 152 (6): 837–848.
- Li, X., Q. Song, W. Liu, H. Rao, S. Xu, and L. Li. 2012. "Protection of Nonpermanent Faults on DC Overhead Lines in MMC-Based HVDC Systems." *IEEE Transactions on Power Delivery* 28 (1): 483–490. <https://doi.org/10.1109/TPWRD.2012.2226249>.
- Malanda, S. C., I. E. Davidson, E. Singh, and E. Buraimoh. 2018. "Analysis of Soil Resistivity and Its Impact on Grounding Systems Design." *Proceedings of the 2018 IEEE PES/IAS PowerAfrica*, Cape Town, South Africa, 324–329. IEEE. June.
- Mansour, D. E. A., M. Numair, A. S. Zalhaf, R. Ramadan, M. M. Darwish, Q. Huang, M. G. Hussien, and O. Abdel-Rahim. 2023. "Applications of IoT and Digital Twin in Electrical Power Systems: A Comprehensive Survey." *IET Generation, Transmission & Distribution* 17 (20): 4457–4479. <https://doi.org/10.1049/gtd2.12940>.
- Micu, D. D., G. C. Christoforidis, and L. Czumbil. 2013. "AC Interference on Pipelines Due to Double Circuit Power Lines: A Detailed Study." *Electric Power Systems Research* 103:1–8. <https://doi.org/10.1016/j.epsr.2013.04.008>.
- Mishra, S., and A. K. Tyagi. 2022. "The Role of Machine Learning Techniques in Internet of Things-Based Cloud Applications." In *Artificial Intelligence-based Internet of Things Systems. Internet of Things*, edited by S. Pal, D. De, and R. Buyya. Cham: Springer. [https://doi.org/10.1007/978-3-030-87059-1\\_4](https://doi.org/10.1007/978-3-030-87059-1_4).
- Mocanu, E., P. H. Nguyen, and M. Gibescu. 2018. "Chapter 7 - Deep Learning for Power System Data Analysis." In *Big Data Application in Power Systems*, edited by Reza Arghandeh and Yuxun Zhou, 125–158. Elsevier. <https://doi.org/10.1016/B978-0-12-811968-6.00007-3>.
- Mohapatra, A. G., A. Mohanty, N. R. Pradhan, S. N. Mohanty, D. Gupta, M. Alharbi, A. Alkhayyat, and A. Khanna. 2023. "An Industry 4.0 Implementation of a Condition Monitoring System and IoT-Enabled Predictive Maintenance Scheme for Diesel 'Generators.'" *Alexandria Engineering Journal* 76:525–541. <https://doi.org/10.1016/j.aej.2023.06.026>.
- Mohapatra, A. G., A. Mohanty, and P. K. Tripathy. 2024. "IoT-Enabled Predictive Maintenance and Analytic Hierarchy Process Based Prioritization of Real-Time Parameters in a Diesel Generator: An Industry 4.0 Case Study." *SN Computer Science* 5 (1): 145. <https://doi.org/10.1007/s42979-023-02508-3>.
- Nassereddine, M. 2024. "Transmission Line Earthing System; Advanced Design Diagram for Safety Compliance." *Electric Power Systems Research* 233:110489. <https://doi.org/10.1016/j.epsr.2024.110489>.
- Nassereddine, M., J. Rizk, A. Hellany, and M. Nagrial. 2013a. "Fault Current Distribution and Pole Earth Potential Rise (EPR) Under Substation Fault." *International Journal of Emerging Electric Power Systems* 14 (5): 499–507. <https://doi.org/10.1515/ijeeps-2012-0034>.
- Nassereddine, M., J. Rizk, A. Hellany, and M. Nagrial. 2013b. "HV Substation Earth Grid Commissioning Using Current Injection Test (CIT) Method." *Proceedings of the 2013 IEEE 8th Conference on Industrial Electronics and Applications (ICIEA)*, Melbourne, VIC, Australia, 67–72. IEEE. June.
- Nassereddine, M., J. Rizk, A. Hellany, and M. Nagrial. 2014a. "ac interference study on pipeline: ohew split

- factor impacts on the induced voltage.” *Journal of Electrical Engineering* 14 (1): 6–6.
- Nassereddine, M., J. Rizk, A. Hellany, and M. Nagrial. 2014b. “Relation Between Transmission Lines Coupling Factor and Over Head Earth Wire Length: Its Impacts on Fault Current Distributions.” *IET Generation, Transmission & Distribution* 8 (4): 600–608. <https://doi.org/10.1049/iet-gtd.2013.0608>.
- Nassereddine, M., J. Rizk, A. Hellany, and M. Nagrial. 2015. “Induced Voltage Behavior on Pipelines Due to HV AC Interference Under Broken OHEW.” *Proceedings of the 2015 IEEE 10th Conference on Industrial Electronics and Applications (ICIEA)*, Auckland, New Zealand, 1408–1413. IEEE. June.
- Nassereddine, M., J. Rizk, M. Nagrial, and A. Hellany. 2015. “HV Substation Earth Grid Commissioning Using Current Injection Test (CIT) Method: Worst Case Scenario Determination.” *International Journal of Energy and Environment* 6 (4): 347.
- Neitzel, D. K. 2016. “Electrical Safety When Working Near Overhead Power Lines.” *ASSE Professional Development Conference and Exposition*, Atlanta, Georgia, USA, ASSE–16. ASSE. June.
- Olowofela, J. A., V. O. Jolaosho, and B. S. Badmus. 2005. “Measuring the Electrical Resistivity of the Earth Using a Fabricated Resistivity Meter.” *European Journal of Physics* 26 (3): 501. <https://doi.org/10.1088/0143-0807/26/3/015>.
- Radhakrishnan, G., and V. Gopalakrishnan. 2020. “RETRACTED: Applications of Internet of Things (IOT) to Improve the Stability of a Grid Connected Power System Using Interline Power Flow Controller.” *Microprocessors and Microsystems* 76:103038. <https://doi.org/10.1016/j.micpro.2020.103038>.
- Sazali, M. S., C. L. Wooi, S. N. M. Arshad, T. S. Wong, Z. Abdul-Malek, and H. Nabipour-Afrouzi. 2020. “Study of Soil Resistivity Using Wenner Four Pin Method: Case Study.” *Proceedings of the 2020 IEEE International Conference on Power and Energy (PECon)*, Penang, Malaysia, 386–391. IEEE. December.
- Shi, Y., R. Zhao, H. Chen, X. Wu, Q. Liu, and Y. Wang. 2020. “A New Design of Generator Set Controller in Cloud Service System Based IoT Technology.” *Proceedings of the IOP Conference Series: Earth and Environmental Science*, Harbin, China, 012067 (Vol. 461). IOP Publishing. April.
- Stracqualursi, E., R. Araneo, and M. Mitolo. 2021. “On the Measuring Methods of the Soil Electrical Resistivity.” *Proceedings of the 2021 IEEE International Conference on Environment and Electrical Engineering and 2021 IEEE Industrial and Commercial Power Systems Europe (EEEIC/I&CPS Europe)*, Bari, Italy, 1–6. IEEE. September.
- Thomas, E. S. 2012. “Bonding Requirements for Conductive Poles.” *Proceedings of the 2012 Rural Electric Power Conference*, Milwaukee, WI, USA, A4–1. IEEE. April.
- Walsh, B. 2005. “Step and Touch Voltage—An Update for 2004.” *Australian Journal of Electrical and Electronics Engineering* 2 (2): 103–116. <https://doi.org/10.1080/1448837X.2005.11464119>.
- Zizzo, G., M. L. Di Silvestre, D. La Cascia, and E. R. Sanseverino. 2015. “A Method for the Evaluation of Fault Current Distribution in Complex High Voltage Networks.” *Electric Power Systems Research* 126:100–110. <https://doi.org/10.1016/j.epsr.2015.05.004>.